

IMECE2005-81837

**MATHEMATICAL MODELING OF THERMAL EFFECTS IN STEADY STATE
DYNAMICS OF MICRORESONATORS USING LORENTZIAN FUNCTION:
PART 1 - THERMAL DAMPING**

G. Nakhaie Jazar¹, Reza.N.Jazar@ndsu.edu

M. Mahinfalah¹, M.Mahinfalah@ndsu.edu

M. R. Aagaah¹, aagaah.rastgaar@ndsu.edu

N. Mahmoudian¹, N.Mahmoudian@ndsu.edu

A. Khazaei², akhazaei@newcomb-boyd.com

M. H. Alimi³, MohammadA@co.fresno.ca.us

¹ Dept. of Mech. Eng., North Dakota State University, Fargo, ND 58105

² Newcomb&Boyd, Consulting Eng. Group, Atlanta, GA 30303-1277

³ County of Fresno, Dept. of Public Works & Planning, Fresno, CA 93721

KEYWORDS: MEMS Dynamics, Microresonators, Thermal Damping

ABSTRACT

Mathematical modeling of thermal effects on steady state dynamics of microresonators, utilizing an analytical approach is studied. Thermal phenomena has two distinct effects, which in this report are called, thermal damping and temperature relaxation. In this part of a two-part report we investigate the thermal damping and its effects on microresonator dynamics. To do this, first the reduced order mathematical model of the system is introduced as a forced mass-spring-damper system, and then a linearized model of electric actuated microbeam resonator is employed. The effect of thermal damping is modeled as an increase in damping rate, utilizing a Lorentzian function of excitation frequency. The steady state frequency-amplitude dependency of the system will be derived utilizing averaging perturbation method. The developed analytic equation describing the frequency response of the system around resonance can be utilized to explain the dynamics of the system, as well as design of dynamic parameters. However, we have focused on exploration of thermal damping.

1. INTRODUCTION

The purpose of this paper is to introduce mathematical modeling and investigate the effect of thermal damping phenomenon in mechanical vibrations with emphasis on dynamic behavior and sensitivity analysis of micro

resonators. So, we develop a mathematical model to describe the thermal damping phenomenon and investigate its effects on MEMS dynamic. To do this the mathematical model of the thermal damping is applied in a forced linear vibrating system to illustrate the thermal damping effects. Then, a linearized model of an electric actuated microbeam resonator will be employed. The effect of thermal damping phenomenon is modeled as an increase in damping rate as a Lorentzian function of excitation frequency. The steady state frequency-amplitude dependency of the system will be derived utilizing averaging perturbation method. The developed analytic equation describing the frequency response of the system around resonance can be utilized to explain the dynamics of the system, as well as resonant frequency and peak amplitude.

The thermal properties of the microbeam material can play a significant role in affecting the design and application of micro systems utilizing a microbeam or microcantilever resonator (Karami and Garnich 2005). The material characteristics affecting vibration behavior of the microresonator are stiffness and damping rates of the microbeam. The energy loss in a micromechanical resonator is measured in terms of the quality factor, defined as $Q = 2\pi e_0 / \Delta e$, where e_0 is the mechanical energy of the resonator and Δe is the energy loss per cycle. The quality factor for a lightly damped single degree of freedom system with damping ratio $\xi \ll 1$ is

approximated by $Q = 1 / (2\xi)$, (Norris and Photiadis 2004).

MEMS devices and systems have been designed by trial and error, mainly because most MEMS devices are modeled using simplified analytical tools, resulting in a relatively approximate prediction of performance behavior. As a result, MEMS design process requires several iterations before the performance requirements of a given device are finally satisfied (Younis, Abdel-Rahman, and Nayfeh 2003, Younis 2004). Conversely, the reduced-order models, known as micromodels, need to be expanded and improved as a tool for prediction and optimization of the proposed behavior. Reduced-order models are developed to capture the most significant characteristics of a MEMS behavior in a few variables (Younis 2004, Nayfeh and Younis 2004).

Most electric actuated MEMS, especially microbeam-based sensors and actuators must work at resonance. Typical microresonator devices employ a parallel capacitor, in which one electrode is fixed and the other is allowed to move using some flexibility. The movable electrode, fabricated in the form of microbeam, microplate, or microcantilever, serves as a mechanical resonator. It is actuated electrically and its motion can be detected by capacitive changes. This motion of the movable electrode can be converted to an electric signal in the capacitance, which is related to the physical quantity being measured (Younis, and Nayfeh 2003).

2. MATHEMATICAL MODELING OF THERMAL DAMPING

Intrinsic sources of dissipation, such as thermoelastic damping, impose a strict upper limit on the attainable quality factors of resonators (Wang et. al. 2000, Hsu et. al. 2001). Thermoelastic damping is the energy dissipation mechanism that is modeled and analyzed in this investigation. Thermoelastic damping is a consequence of the microbeam being in thermal equilibrium with its environment. This damping depends on the thermodynamic properties of the material which are functions of temperature. Thermoelastic damping is proportional to frequency; hence, when the principal natural frequency moves up while the size of devices decreases, the thermoelastic damping becomes more significant (Lifshitz and Roukes 2000). Temperature changes lead to irreversible heat flow and to entropic dissipation. In other words, thermal energy dissipation is

caused by irreversible heat flow across the thickness of the microcantilever as it oscillates (Yasumura et. al. 2000).

Material linear thermal expansion coefficient $\alpha_T = (1/L)(\partial L / \partial T)$ is the macroscopic parameter that couples changes in length (strain) with changes in temperature. Zener was the first researcher who investigated and modeled the effect of internal frictions in resonating thermoelastic solids known as “thermoelastic damping” (Zener 1937, 1938a, 1938b, 1947). According to Zener approximate theory, the “thermoelastic damping is significant when the frequency of vibration ω , satisfies the condition $\omega\tau_Z = 1$, where, $\tau_Z = a^2 / (\pi^2\gamma_T)$ is the Zener relaxation time, a is the thickness of the microbeam, and γ_T is the thermal diffusivity of the microbeam material (Zener, Otis, and Nuckolls 1938). Zener relaxation time τ_Z , is related to the quality factor due to the following relationship

$$Q_z^{-1} = \frac{E\alpha_T^2 T_0}{C_p} \frac{\omega\tau_Z}{1 + (\omega\tau_Z)^2} \quad (1)$$

where, C_p is the heat capacity per unit volume of the beam material, T_0 is the uniform temperature of the beam, and E is Young modulus. In fact, the expression (1) is the leading term in an infinite series which is well approximated by the single term (Norris and Photiadis 2004, Zener 1937).

A better approximation for Equation (1) is provided by Alblas (1961, 1968), and Lifshitz and Roukes (2000). The natural or eigen frequencies for microbeams in terms of the beam dimensions are $\omega_i = a_i^2 \pi^2 \sqrt{EI / (\rho L^4)}$ where, I is the area second moment of inertia of the cross section, ρ is the mass per unit length of the beam, and a_i is a number depending on the boundary conditions (Meirovitch 1997). Equation (1) can be approximated by the following equation with less than 1% error

$$Q^{-1} = \frac{E\alpha_T^2 T_0}{C_p} \mathcal{L}\left(\frac{\xi^2}{\pi^2/2}\right), \quad \mathcal{L}(x) = \frac{x}{1+x^2} \quad (2)$$

where \mathcal{L} is the Lorentzian function and $\xi^2 = a_i^2 \pi^2 b^2 / (4\sqrt{3}L^2 l_T)$, where $l_T = \gamma\sqrt{\rho/E}$ is thermal diffusion length. The values of l_T is measured experimentally for the material of the beam and are tabulated. (Lifshitz and Roukes 2000; Gough 1968). Lorentzian function (shown in Figure 1)

has been derived and used in thermal-loss analysis especially in flexural beam resonators by most of researchers (Srikanth and Senturia 2002, Yang et al, 2002; Abdolvand et al, 2003; Jeong et al, 2003; De and Aluru 2004; Fejer et al, 2004; Husman et al, 2004).

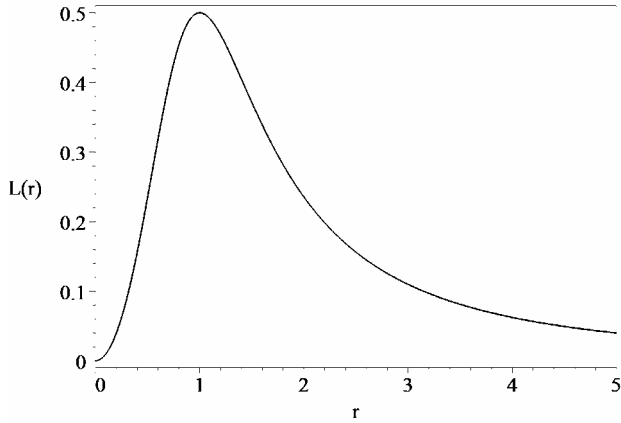


Figure 1. Lorentzian function

For a linear mass-spring-dashpot oscillator, the quality factor Q , is defined by $Q = \sqrt{km}/c$. Therefore, employing (1) and (2), we introduce a frequency-dependent force

$$f_{Td} = c_T \mathcal{L}\left(\frac{\omega^2}{\omega_l^2}\right) \dot{z} \quad (3)$$

to simulate the damping force corresponding to thermal damping. The coefficient c_T defines the thermal damping per unit length of the microbeam which depends on geometric and material properties of the microbeam and must be determined experimentally. Thermal damping force introduces a new variable within the equation of motion, and it is a function of excitation frequency with a maximum at fundamental resonance frequency. In other words, the thermal damping is modeled by a viscous damping with a Lorentzian frequency-dependent coefficient.

Employing (3) indicates that the damping exhibit a broad maximum at natural frequency ω_l . This is in agreement with the classic phenomenon called anelasticity (Zener 1947; Saulson 1990).

3. THERMAL DAMPING EFFECT IN SINGLE DOF VIBRATING SYSTEMS

Consider the vibration isolation system shown in Figure 2. The base experiences a harmonic excitation displacement $y = Y \sin(\omega t)$. Overall damping of the system is a combination of viscous damping c and the thermal damping $c_T (\omega/\omega_l)^2 / (1 + (\omega/\omega_l)^4)$.

Therefore, the equation of motion of the system is

$$m\ddot{x} + \left(c + c_T \frac{(\omega/\omega_l)^2}{1 + (\omega/\omega_l)^4} \right) (\dot{x} - \dot{y}) + k(x - y) = 0 \quad (4)$$

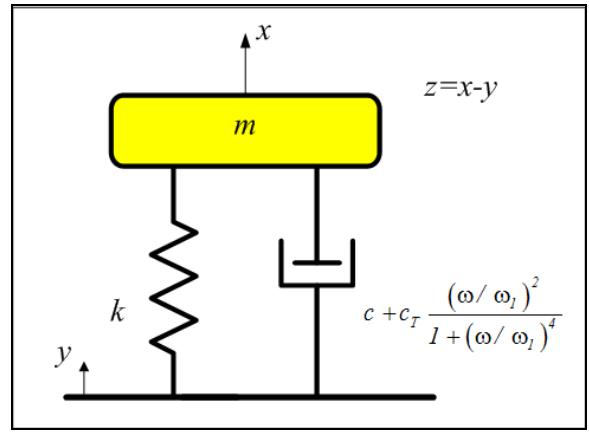


Figure 2. Lorentzian function

Introducing a relative displacement coordinate $z = x - y$, and employing a set of dimensionless parameters, the equation of motion transforms to the following equation,

$$u'' + \left(a_1 + a_2 \frac{r^2}{1 + r^4} \right) u' + u = r^2 \sin(r\tau) \quad (5)$$

where

$$\begin{aligned} x - y = z \quad \frac{z}{Y} = u \quad \omega_l = \sqrt{\frac{k_l}{m}} \quad \omega_l t = \tau \\ r = \frac{\omega}{\omega_l} \quad a_1 = \frac{c}{\sqrt{k_l m}} \quad a_2 = \frac{c_T}{\sqrt{k_l m}} \end{aligned} \quad (6)$$

It can be shown that the steady state solution of (5) is

$$\begin{aligned} U = r^2 (1 + r^4) \left[r^{12} + (a_1^2 - 2)(r^{10} + r^2) \right. \\ \left. + (2a_1 a_2 + 3)(r^8 + r^4) + (2a_1^2 + a_2^2 - 4)r^6 + 1 \right]^{-1/2} \quad (7) \end{aligned}$$

Figures 3 and 4 show the frequency response of the system without and with thermal damping, respectively. More specifically, in Figure 3, $a_2=0$, and in Figure 4, $a_2=0.1$. The a_1 is indicator of individual curve with values from zero to one, and increment of 0.1 . As expected, increasing a_1 decreases the amplitude in both figures. Because of small value of a_2 the difference between these figures is not obvious.

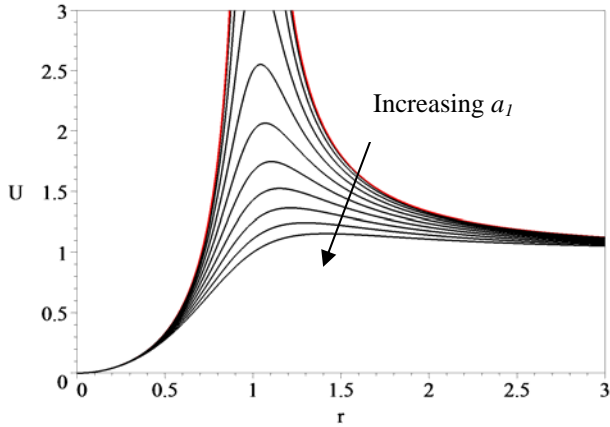


Figure 3. U for $a_2=0$ and $a_1=0,0.1,\dots,1.0$.

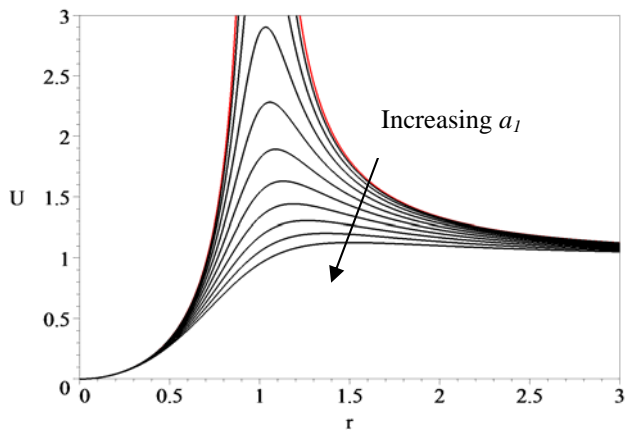


Figure 4. U for $a_2=0.1$ and $a_1=0,0.1,\dots,1.0$.

To show the difference, in Figure 5 we kept $a_1=0.4$ and plotted U for $a_2=0$ and $a_2=0.1$. The upper curve corresponds to no thermal damping while the lower curve is for $a_2=0.1$. Figure 5 clearly shows that thermal damping has maximum effect at resonant frequency.

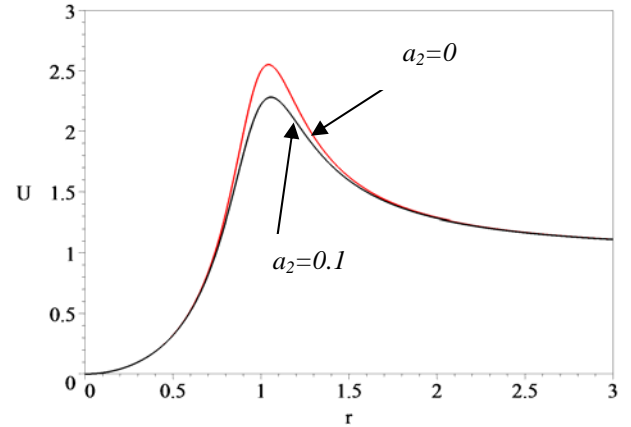


Figure 5. U for $a_1=0.4$ and $a_2=0, 0.1$.

4. REDUCED ORDER MODEL OF MICRORESONATORS

The microresonator is composed of a beam resonator, a ground plane underneath in contact with the beam, and one (or more) capacitive transducer electrode(s). To bias and excite the device, a DC-bias voltage, v_p , is applied to the resonator while an AC excitation voltage is applied to its underlying ground plane(s). A variable capacitor model on a clamped-clamped microbeam and a microcantilever are illustrated in Figure 6. The electric load actuation is achieved by applying a voltage difference between opposite electrodes of a variable capacitor. The induced electrostatic force deforms the capacitor until they are balanced by the restoring mechanical forces. The electric load is composed of a DC polarization voltage, v_p , and an AC actuating voltage, $v = v_i \sin(\omega t)$. The polarization voltage has an upper limit called “collapse” load, beyond which the mechanical restoring force can no longer resist its opposing force (Hsu 2002).

The one dimensional electrostatic force, f_e , between two electrodes is

$$f_e = \frac{\epsilon_0 A (v - v_p)^2}{2(d - w_0)^2}, \quad v = v_i \sin(\omega t) \quad (8)$$

where, $\epsilon_0 = 8.85 \times 10^{-12} \text{ As/Vm}$ is permittivity in vacuum, A is the area of the microplate, and $w=w(x,t)$ is the lateral displacement of the microbeam (Hsu 2002).

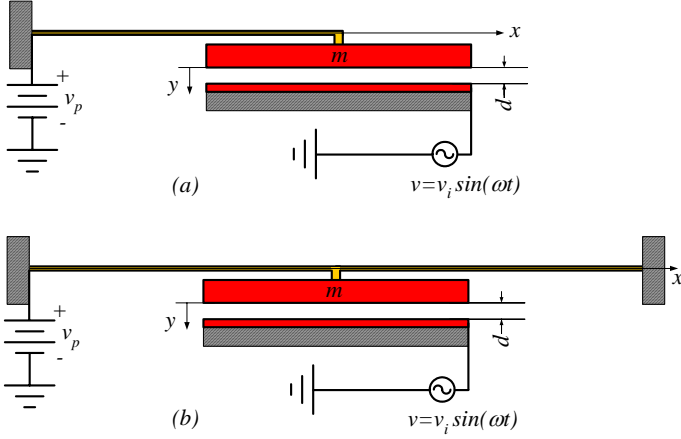


Figure 6. A microcantilever and a clamped-clamped microbeam model of microresonators.

When the excitation has a frequency close to the fundamental resonance frequency of the resonator, the resonator begins to oscillate, creating a time varying capacitance $C = \epsilon_0 A / (d - w)$ between the resonator and the electrode. It is usually assumed that the beam length is much greater than the electrode lengths. Therefore, the variation of the beam deflection across the length of the electrodes is ignorable (Nguyen 1995).

The equation describing lateral vibrations of the microbeam can be summarized and simplified to the following equation when the beam's geometry is uniform.

$$\rho \frac{\partial^2 w}{\partial t^2} + c \frac{\partial w}{\partial t} + EI \frac{\partial^4 w}{\partial x^4} + c_T \frac{(\omega / \omega_1)^2}{1 + (\omega / \omega_1)^4} \frac{\partial w}{\partial t} = \frac{\epsilon_0 A (v - v_p)^2}{2(d - w_0)^2} \quad (9)$$

To make the equation of motion dimensionless the following variables are defined. The parameter n is a constant depending on mode shape of the microbeam.

$$\begin{aligned} \tau = \omega_1 t \quad \omega_1 &= \frac{n^2}{L^2} \sqrt{\frac{EI}{\rho}} \quad z = \frac{x}{L} \\ y = \frac{w}{d} \quad Y = \frac{w_0}{d} \quad r = \frac{\omega}{\omega_1} \quad a_1 &= \frac{cL^2}{n\sqrt{\rho EI}} \quad (10) \\ a_2 &= \frac{c_T L^2}{n\sqrt{\rho EI}} \quad a_4 = \frac{\epsilon_0 AL^4}{2n^2 d^3 EI} \end{aligned}$$

Using these parameters, the equation of motion transforms to the following dimensionless equation.

$$\frac{\partial^2 y}{\partial \tau^2} + a_1 \frac{\partial y}{\partial \tau} + \frac{\partial^4 y}{\partial z^4} + a_2 \frac{r^2}{1 + r^4} \frac{\partial y}{\partial \tau} = a_4 \frac{(v - v_p)^2}{(1 - Y)^2} \quad (11)$$

We apply a separation solution

$$y = Y(\tau) \cdot \varphi(z) \quad (12)$$

where the spatial function $\varphi(z)$ is called mode shape function, and must satisfy the boundary conditions. By accepting a first harmonic shape function, the temporal function $Y(\tau)$ would then represent the maximum deflection of the microbeam, which is the middle point for symmetric boundary conditions, and the tip point for microcantilever.

A microcantilever is a microbeam with the following boundary conditions.

$$\begin{aligned} y(0, \tau) = 0 \quad \frac{\partial y}{\partial z} y(0, \tau) \\ \frac{\partial^2 y}{\partial z^2} y(L, \tau) = 0 \quad \frac{\partial^3 y}{\partial z^3} y(L, \tau) = 0 \end{aligned} \quad (13)$$

The first harmonic mode shape satisfying the required boundary conditions, is

$$\varphi(x) = \cos\left(\frac{\pi x}{2}\right). \quad (14)$$

and the mode shape parameter is

$$n = \frac{\pi^2}{4}. \quad (15)$$

Therefore, the required differential equation for the temporal function $Y(\tau)$ related to a microcantilever, would be

$$\begin{aligned} \ddot{Y} + \left(h + a_2 \frac{r^2}{1 + r^4} \right) \dot{Y} + Y = \frac{I}{(1 - Y)^2} \\ \times \left[(\alpha + \beta) + 2\sqrt{2\alpha\beta} \sin(r\tau) - \beta \cos(2r\tau) \right] \end{aligned} \quad (16)$$

where,

$$h = a_1 \quad \alpha = a_4 v_p^2 \quad 2\sqrt{2\alpha\beta} = 2a_4 v_p v_i \quad \beta = \frac{a_4}{2} v_i^2. \quad (17)$$

Assuming $y \ll 1$, the linearized governing equation of the microresonator to analyze the thermal damping, would be

$$\ddot{Y} + \left(h + a_2 \frac{r^3}{1+r^4} \right) \dot{Y} + 2 \left(\frac{I}{2} - \beta - \alpha + \beta \cos(2r\tau) - 2\sqrt{2\alpha\beta} \sin(2r\tau) \right) Y \quad (18)$$

$$= \alpha + 2\beta \sin^2(r\tau) + 2\sqrt{2\alpha\beta} \sin(r\tau)$$

with equilibrium at

$$A_0 = \frac{\alpha + \beta}{1 - 2\alpha - 2\beta}. \quad (19)$$

5. THERMAL DAMPING EFFECT IN MICRORESONATORS

To find the amplitude of oscillation of the microbeam around resonance and considering the initial displacement due to polarization, we assume a solution in the following form

$$y = A_0 + A(\tau) \sin(r\tau + \psi(\tau)) \quad (20)$$

$$y' = A(\tau) r \cos(r\tau + \psi(\tau)) \quad (21)$$

It can be shown that eliminating secular terms requires that

$$A_0 = \frac{\alpha + \beta}{1 - 2\alpha - 2\beta}. \quad (22)$$

while applying multiple time scale method produces the following relationship between the parameters of the system to have a periodic steady state response with frequency r .

$$\begin{aligned} & Z_1 r^{12} + Z_2 r^{10} + Z_3 r^9 + Z_4 r^8 + Z_5 r^7 \\ & + (Z_6 - Z_7 \sqrt{Z_8}) r^6 + Z_9 r^5 \\ & + (Z_{10} - Z_{11} \sqrt{Z_8}) r^4 + Z_{12} r^3 \\ & + (Z_{13} - Z_{11} \sqrt{Z_8}) r^2 + Z_{15} - Z_{16} \sqrt{Z_8} = 0 \end{aligned} \quad (23)$$

where

$$Z_1 = 4\beta^2 A^4 \quad (24)$$

$$Z_2 = 4\beta^2 A^4 (4\beta + 2 + 4\alpha + h^2) \quad (25)$$

$$Z_4 = 8\beta^2 A^4 h a_2 \quad (26)$$

$$\begin{aligned} Z_4 &= 4\beta^2 A^4 (-1 + 42\alpha + 4h^2 + 4\alpha^2) \\ &+ 4\beta^3 A^4 (3\beta + 8\alpha + 12) \\ &- 16\alpha\beta^3 A^2 (4A_0(A_0 + 1) + 1) \end{aligned} \quad (27)$$

$$Z_5 = 24\beta^2 A^4 h a_2 \quad (28)$$

$$\begin{aligned} Z_6 &= 4\beta^2 A^4 [8\alpha(\alpha + 1) + 2(3h^2 - 2) + 2a_2^2] \\ &- 64\alpha\beta^3 A^2 [4A_0(A_0 + 1) + 1] \end{aligned} \quad (29)$$

$$Z_7 = 16\beta^2 A^2 (A_0 + 1) \quad (30)$$

$$\begin{aligned} Z_8 &= \alpha^2 \beta^2 (1 + r^2)(2A_0 + 2) \\ &- \alpha\beta^2 A^2 (1 + r^2)((1 + r^2)(\beta + 2\alpha) + r^4 - 1) \end{aligned} \quad (31)$$

$$Z_9 = Z_5 \quad (32)$$

$$\begin{aligned} Z_{10} &= 4\beta^5 A^4 (18\beta + 8(6\alpha - 1)) \\ &+ 4\beta^2 A^4 [8\alpha(2\alpha - 1) + 4h^2 - 1 + a_2^2] \\ &- 96\alpha\beta^3 A^2 [4A_0(A_0 + 1) + 1] \end{aligned} \quad (33)$$

$$Z_{11} = 48\beta^2 A^2 (2A_0 + 1) \quad (34)$$

$$Z_{12} = Z_4 \quad (35)$$

$$\begin{aligned} Z_{13} &= 4\beta^4 A^4 (12\beta + 4(8\alpha - 3)) \\ &+ 4\beta^2 A^4 [4\alpha(4\alpha - 3) + h^2 + 2] \\ &- 64\alpha\beta^3 A^2 [4A_0(A_0 + 1) + 1] \end{aligned} \quad (36)$$

$$\begin{aligned} Z_{15} &= 4\beta^2 A^4 [\beta(4\beta + 4(2\alpha - 1)) + 4\alpha(\alpha - 1) + 1] \\ &- 16\alpha\beta^3 A^2 [4A_0(A_0 + 1) + 1] \end{aligned} \quad (37)$$

$$Z_{16} = \frac{Z_{11}}{3} \quad (38)$$

6. DYNAMIC ANALYSIS

Equation (23) describes the frequency behavior of the microresonator indicating that its dynamics is governed by polarization voltage parameter α , alternative excitation voltage parameters β , damping parameter h , the excitation frequency ratio r , as well as the thermal damping parameters a_2 . In order to demonstrate the dependency of steady state behavior of the MEMS, we graphically illustrate the frequency response for various parameters

utilizing Table 1 that indicates the nominal values of a sample micrcantilever resonator (Kanda et al, 2000; Yang et al 2002; Khaled et al, 2003; Kaajakari et al, 2004).

Table 1. Nominal parameters of the microresonator.

m	$1 \times 10^{-11} \text{ kg}$
c	$1 \times 10^{-8} \text{ Ns / m}$
k	1 N/m
d	$2.0 \text{ } \mu\text{m}$
α	$0.0000553125 v_p^2$
A	$200 \times 50 \text{ } \mu\text{m}$
β	$0.00002765625 v_i^2$

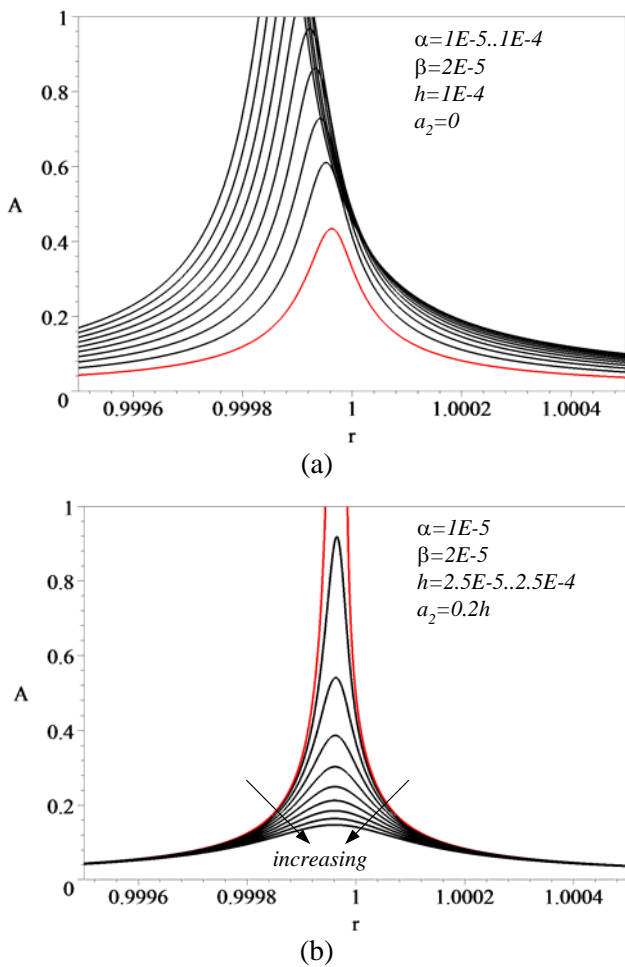


Figure 7. Effect of variation of polarization voltage.

Figure 7 depicts the effect of variation of polarization voltage for a set of parameters. The amplitude of steady state oscillation increases by increasing the polarization voltage. No thermal damping is shown in Figure 7(a) where a_2 is set to zero. Thermal damping increases the damping of the system near resonance, and hence diminishes the resonance amplitudes but has almost no effect on the off resonance responses as shown in Figure 7(b). The value of thermal damping is set to 20% of the nominal value of linear damping of the system. The peak value of the frequency response at resonance is a monotonically increasing function of the polarization voltage. Therefore, there must be a maximum acceptable α , due to constraint $Y < 1$.

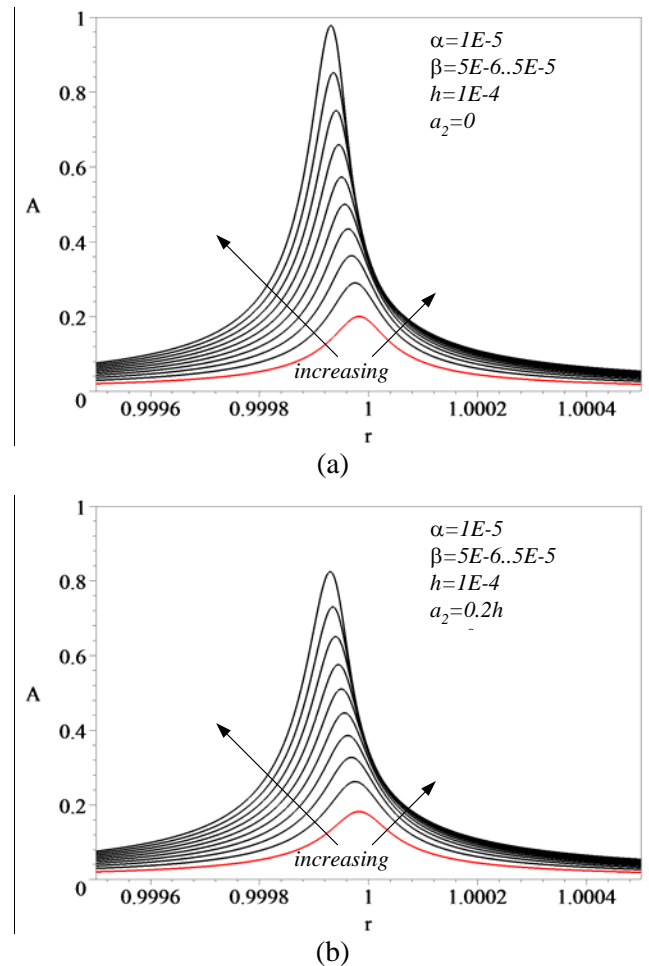


Figure 8. Effect of variation of excitation voltage.

The response of the system to variation of the excitation voltage has the same pattern as polarization voltage. More specifically, the peak value increases and the resonant

frequency shifts to lower frequencies when the amplitude of the excitation voltage increases. Thermal damping also has the same effects as described for polarization voltage variation. There is also a higher limit for the alternative voltage to have oscillation within the gap size limit. Variation of excitation voltage is shown in Figure 8.

The resonance frequency is a very important parameter in resonator-based microsensors. The resonance frequency also indirectly affects design parameters (Sudipo and Aluru 2004). To determine the capability of the MEMS to sense a shift in resonance frequency by varying a parameter, the Equation (23) must be investigated numerically.

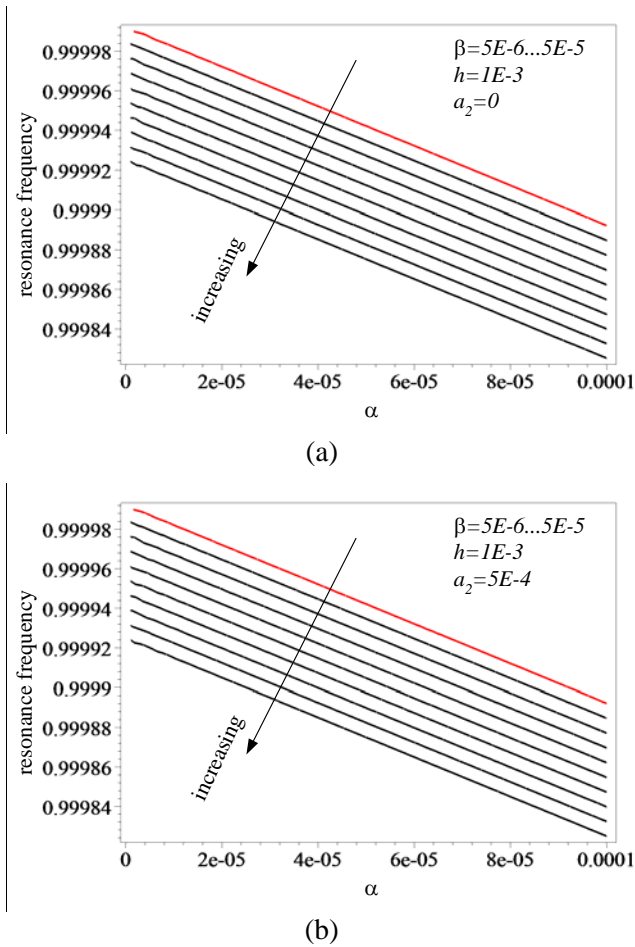


Figure 9. Effect of variation of excitation and polarization voltages on shift of resonance.

Shift of resonance frequency, r_0 , are illustrated in Figures 9 and 10. First, the thermal coefficients a_2 is set to zero and the result is shown in Figure 9(a). The resonance frequency is monotonically decreasing function of

increasing both polarization and excitation voltages. Within the limit of possible variation of voltages according to the physical limit of gap, the behavior of resonance shifting looks linear with variation of both voltages. However, introducing thermal damping destroys the linearity of the resonant frequency and excitation voltages relationship, although it is still a decreasing function (Figure 9(b)).

The behavior of resonant frequency is not linear nor monotonic when damping is varied (Figure 10). Figure 10(a) depicts the effect of variation of damping and polarization voltage on resonant shift when the thermal damping is eliminated. The resonance frequency is sensitive when damping is low. However, its sensitivity disappears shortly. Resonance frequencies are compared in Figure 10(b) for thermal damping.

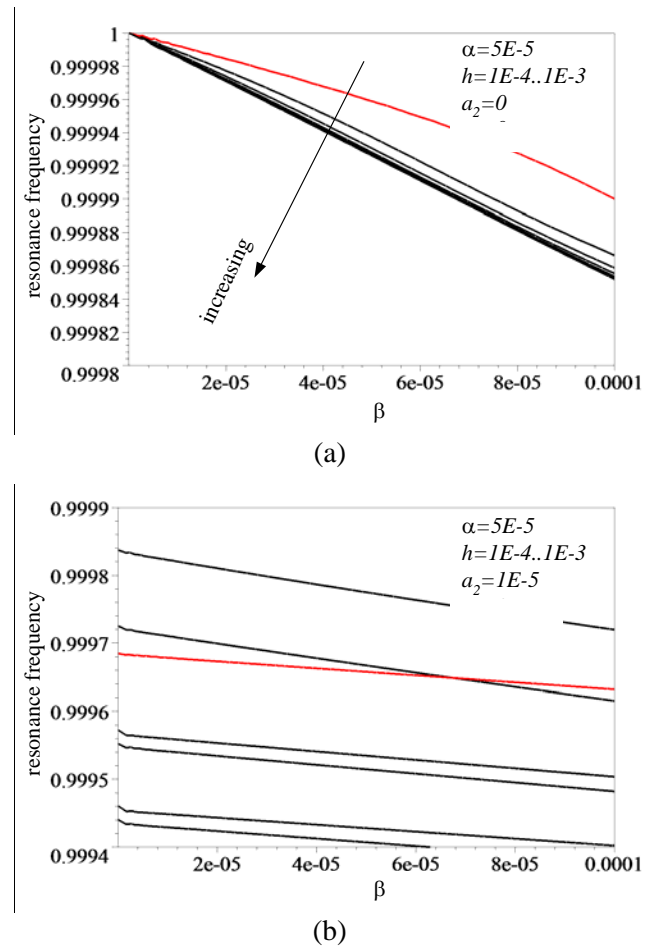


Figure 10. Effect of the variation of damping and excitation voltage on shift of resonance.

7. CONCLUSION

We have modeled and analyzed the effects of thermal damping in a single dof vibrating system as well as electric actuated microresonator. The thermal damping has been defined by an effective force per unit length of the vibrating microbeam. Thermal damping is due to warming and heat energy dissipation and is frequency dependent. The thermal damping is described by a suitable Lorentzian function of excitation frequency with a maximum at the resonance frequency of the system.

Employing a set of dimensionless variables, equation of flexural motion of the microbeam has been derived including thermal damping modeling. The steady state response of the system has been analyzed employing multiple scale perturbation method. Frequency responses and resonant frequency shifting of vibration have been investigated by varying dynamic parameters involved. Thermal damping has a reduction effect on peak amplitude.

REFERENCES

- Abdolvand R., Ho G.K., Erbil A., and Ayazi F., (2003), "Thermoelastic damping in ternech-refilled polysilicon resonators", *The 12th International Conference on Solid State Sensors, Actuators and Microsystems, Boston, USA, June 8-12*.
- Alblas, J. B., (1961), "On the general theory of thermoelastic friction", *Appl. Sci. Res. A10*, 349–362.
- Alblas, J. B., (1981), "A note on the theory of thermoelastic damping", *J. Thermal Stresses*, 4, 333–355.
- Barmatz M., and Chen H.S., (1974), "Young's modulus and friction in metallic glass alloys from 1.5 to 300 K", *J. Physical Review B*, 9(10), 4073-4083.
- De S.K., and Aluru N.R., (2004), "Full-Lagrangian schemes for dynamic analysis of electrostatic MEMS", *Journal of Microelectromechanical Systems*, 11(5), 737-758.
- Fejerl M.M., Rowan S., Cagnoli G., Crooks D.R.M., Gretarsson A., Harry G.M., Hough J., Penn S.D., Sneddon P.H., and Vyatchanin S.P., "Thermoelastic dissipation in inhomogeneous media: loss measurements and displacement noise in coated test masses for interferometric gravitational wave detectors", *arXiv:gr-qc/0402034 v1 6 Feb 2004, 1-42*.
- Gough W., (1968), "The graphical analysis of a Lorentzian function and a differentiated Lorentzian function", *J. Physical Review A*, 2(1), 704-709.
- Gysin U., Rast S., Meyer E., Lee D.W., Vettiger P., and Gerber C., (2004), "Temperature dependence of the force sensitivity of silicon cantilevers", *Physical Review B*, 69, 045403, 1-6.
- Hsu, T.R., (2002), "MEMS & Microsystems Design and Manufacture", McGraw Hill, New York.
- Hsu, W. T., Clark, J. R., and Nguyen C. T., (2001), "Q-optimized lateral free-free beam micromechanical resonators," *Proc. 11th International Conference on Solid-State Sensors and Actuators (Transducers '01), Munich, Germany, pp. 1110–1113*.
- Husman M.E., Hough J., and Robertson N.A., (2004), "Thermal noise in a pendulum suspended by multiple wires", *Class. Quantum Grav.* 21, 1371–1381.
- Jeong J., Chung S., Lee S.H., and Kwon D., (2003), "Evaluation of elastic properties and temperature effects in Si thin film using an electrostatic microresonator", *Journal of Microelectromechanical Systems*, 12(4), 524-530.
- Kanda T., Morita T., Kurosawa M.K., and Higuchi T., (2000), "A flat type touch probe sensor using PZT thin film vibrator", *Sensors and Actuators* 83, 67-75.
- Karami G., and Garnich, M., "Micromechanical study of thermoelastic behavior of composites with periodic fiber wariness", *Journal of Composites B*, 36, 241-248, 2005.
- Khaled A.R.A., Vafai K., Yang M., Zhang X., and Ozkan C.S., (2003), "Analysis, control and augmentation of microcantilever deflections in bio-sensing systems", *Sensors and Actuators B*.
- Lifshitz, R., and Roukes, M., L., (2000), "Thermoelastic damping in micro- and nanomechanical systems", *Physical Review*, 61(8), 5600-5609.
- Meirovitch, L., (1997), "Principles and technologies of vibrations", Prentice Hall.
- Nayfeh, A. H., and Younis, M. I., (2004), "A new approach to the modeling and simulation of flexible microstructures under the effect of squeeze-film damping", *Journal of Micromechanics and Microengineering*, 14, 170-181.
- Nguyen, C., T., C., (1995), "Micromechanical resonators for oscillators and filters", *Proc., IEEE International Ultrasonic Symposium, Seattle, WA, pp. 489-499, Nov. 7-10*.
- Norris, A. N., and Photiadis, D. M., (2004), "Thermoelastic relaxation in elastic structures, with

- applications to thin plates”, *arXiv:cond-mat/0405323*, v2, Nov. 2004, 1-22.
- Saulson, P. R., “Thermal noise in mechanical experiments”, *Physical Review D*, 42(8), 2437-2445, 1990.
- Srikanth V.T., Senturia S.D., (2002), “Thermoelastic damping in fine-grained polysilicon flexural beam resonators”, *J. Microelectromech. Syst.*, 11 (5), 499–504.
- Sudipo K, and Aluru N.R., (2004), “Full-Lagrangian schemes for dynamic analysis of electrostatic MEMS”, *Journal of Microelectromechanical Systems*, 13(5), 737-758.
- Wang, K., Wong, A. C., and Nguyen C. T., (2000), “VHF free-free beam high-Q micromechanical resonators,” *Journal Microelectromech. Syst.*, 9, pp. 347–360.
- Yang J. L., Ono T., and Esashi M., (2002), “Energy dissipation in submicrometer thick singlecrystal silicon cantilevers”, *J. Microelectromech. Sys.*, 11, 775–783.
- Yang J., Ono T., and Esashi M., (2002), “Energy dissipation in submicrometer thick single-crystal silicon cantilevers”, *Journal of Microelectromechanical Systems*, 11(6), 775-783.
- Yasymura, K. Y., Stowe, T. D., Chow, E. M., Pfafman, T., Kenny, T. M., Stipe, B. C., and Rugar, D., “Quality factors in micron- and submicron-thick cantilevers”, *Journal of Microelectromechanical Systems*, 9(1), 117-125, 2000.
- Younis, M. I., and Nayfeh, A. H., (2003), “A study of the nonlinear response of a resonant microbeam to electric actuation”, *Journal of Nonlinear Dynamics*, 31, 91-117.
- Younis, M., I., (2004), “Modeling and Simulation of Micrielectromechanical System in Multi-Physics Fields”, *Ph.D., thesis, Mechanical Engineering, Virginia Polytechnic Institute and State University*.
- Younis, M., I., Abdel-Rahman, E., M., Nayfeh, A., (2003), “A Reduced-Order Model for Electrically Actuated Microbeam-Based MEMS”, *Journal of Microelectromechanical Systems*, 12(5), 672-680.
- Zalalutdinov V., Mattila T., Oja A., and Seppa H., (2004), “ Nonlinear limits for single-crystal silicon microresonators”, *Journal of Microelectromechanical Systems*, 13(5), 715-724.
- Zener, C., (1937), “Internal friction in solids, I. Theory of internal friction in reeds”, *Physical Review*, 52, 230-235.
- Zener, C., (1938a), “Internal friction in solids, II. General theory of thermoelastic internal friction”, *Physical Review*, 53, 90-99.
- Zener, C., (1938b), “Internal friction in solids, IV. Relation between cold work and internal friction”, *Physical Review*, 53, 582-586.
- Zener, C., (1948), “*Elasticity and anelasticity of metals*”, University of Chicago Press, Chicago.
- Zener, C., Otis, W., and Nuckolls, R., (1938), “Internal friction in solids, III. Experimental demonstration of thermoelastic internal friction”, *Physical Review*, 53, 100-101.